Altered intracellular calcium homeostasis and endoplasmic reticulum redox state in *Saccharomyces cerevisiae* cells lacking Grx6 glutaredoxin

Judit Puigpinós, Celia Casas, and Enrique Herrero
Departament de Ciències Mèdiques Bàsiques, Universitat de Lleida, IRBLleida, 25198 Lleida, Spain

ABSTRACT **Glutaredoxin 6 (Grx6) of *Saccharomyces cerevisiae* is an integral thiol oxidoreductase protein of the endoplasmic reticulum/Golgi vesicles. Its absence alters the redox equilibrium of the reticulum lumen toward a more oxidized state, thus compensating the defects in protein folding/secretion and cell growth caused by low levels of the oxidase Ero1. In addition, null mutants in *GRX6* display a more intense unfolded protein response than wild-type cells upon treatment with inducers of this pathway. These observations support a role of Grx6 in regulating the glutathionylation of thiols of endoplasmic reticulum/Golgi target proteins and consequently the equilibrium between reduced and oxidized glutathione in the lumen of these compartments. A specific function influenced by Grx6 activity is the homeostasis of intracellular calcium. Grx6-deficient mutants have reduced levels of calcium in the ER lumen, whereas accumulation occurs at the cytosol from extracellular sources. This results in permanent activation of the calcineurin-dependent pathway in these cells. Some but not all the phenotypes of the mutant are coincident with those of mutants deficient in intracellular calcium transporters, such as the Golgi Pmr1 protein. The results presented in this study provide evidence for redox regulation of calcium homeostasis in yeast cells.**

Monitoring Editor
Benjamin S. Glick
University of Chicago

Received: Jun 19, 2014
Revised: Oct 10, 2014
Accepted: Oct 22, 2014

INTRODUCTION

Ion homeostasis is essential for the physiology of the cell. Cations such as K^+, Na^+, or Ca^{2+} are required for a large diversity of cellular processes, but at the same time they must be kept at appropriate intracellular concentrations to avoid toxicity. The yeast *Saccharomyces cerevisiae* has been used as a model to study the plasma membrane and intracellular transport mechanisms contributing to maintain cation homeostasis, as well as the responses to restore such homeostasis when this is disturbed (Ariño *et al.*, 2010; Cunningham, 2011; Cyert and Philpott, 2013).

Cytosolic Ca^{2+} concentration is important in signaling and regulation of many essential responses in practically all cell types (Clapham, 2007). To make this signaling possible, cells maintain cytosolic calcium at low levels and have different transporters that regulate the concentration of this cation in the intracellular compartments, causing the oscillations required for cell signaling. In yeast cells, the vacuole is the major Ca^{2+} store. Entry or exit of the cation from this organelle is mediated by different transporters (reviewed by Cunningham, 2011). Pmc1 is a vacuolar Ca^{2+} pump related to the PMCA family of plasma membrane Ca^{2+} ATPases from mammals and plants and is the main contributor to vacuolar Ca^{2+} levels. These also become determined by the activities of the Ca^{2+}/H^+ exchanger Vcx1 and the Ca^{2+} channel Yvc1, which respectively import or release Ca^{2+} into or from the vacuole. As in mammalian cells, in yeast cells, Ca^{2+} is required at the endoplasmic reticulum (ER) for the correct function of the protein folding and secretory machinery (Bonilla *et al.*, 2002). Adequate Ca^{2+} levels at the ER/early Golgi organelles mainly result from the activity of Pmr1, a P-type Ca^{2+}/Mn^{2+} pump of the SPCA family that imports those cations into the organelle lumen (Antebi and Fink, 1992; Dürr *et al.*, 1998). Spf1/Cod1 is another P-type ATPase that acts synergistically with Pmr1 in transporting Ca^{2+} into the ER lumen (Cronin *et al.*, 2002) and also influences entry of Mn^{2+} inside ER vesicles (Cohen *et al.*, 2013). Recently, Gdt1/Grc1 was characterized as a Golgi-localized transmembrane member of

This article was published online ahead of print in MBoC in Press (http://www.molbiolcell.org/cgi/doi/10.1091/mbc.E14-06-1137) on October 29, 2014.

Address correspondence to: Enrique Herrero (enric.herrero@cmb.udl.cat).

Abbreviations used: CPY, carboxypeptidase Y; DTT, dithiothreitol; ER, endoplasmic reticulum; GRX, glutaredoxin; GSH, reduced glutathione; UPR, unfolded protein response.

the cation/Ca^{2+} exchanger superfamily that would contribute together with Pmr1 for Ca^{2+} supply to the Golgi apparatus in yeast (Demaegd *et al.*, 2013). On the other hand, it has been proposed that Csg2 acts as a channel that releases Ca^{2+} from ER to cytosol to keep with luminal ER homeostasis (Beeler *et al.*, 1994; Tanida *et al.*, 1996). At the *S. cerevisiae* plasma membrane, two mechanisms operate for Ca^{2+} influx—the low-affinity system (which acts only in Ca^{2+}-rich conditions) and the high-affinity system (HACS; acting in both Ca^{2+}-rich and -poor conditions). HACS is composed of three interacting proteins (Cch1, Mid1, and Ecm7) with homology to the voltage-gated Ca^{2+} channels in animals (Cunningham, 2011).

The mentioned Ca^{2+} transport systems are interrelated. Thus the absence of Pmr1, which lowers Ca^{2+} levels at the lumen of ER/Golgi compartments, activates HACS; consequently, cytosolic calcium levels increase, and this leads the cell to induce the calcineurin-dependent pathway (Locke *et al.*, 2000; Bonilla and Cunningham, 2003). In yeast, this pathway responds to alterations in intracellular Ca^{2+} and also to high environmental concentrations of cations such as Ca^{2+} or Na^{+} and to sexual pheromones (Cyert, 2003; Thewes, 2014). Central in this pathway is the calmodulin/Ca^{2+} complex, which activates the Ser/Thr phosphatase calcineurin, which in turn dephosphorylates the Crz1 transcription factor, causing its import to the nucleus. Crz1 targets promoter elements with the CDRE motif. In this way, calcium and sodium stresses share common Crz1-dependent gene targets (Yoshimoto *et al.*, 2002). *PMC1* is one of the genes up-regulated upon alteration of Ca^{2+} homeostasis (Yoshimoto *et al.*, 2002). Thus a Δ*pmr1* mutant accumulates a large amount of Ca^{2+} at the vacuole (Halachmi and Eilam, 1996) as a compensatory mechanism, and a Δ*pmr1*Δ*pmc1* mutant is nonviable (Cunningham and Fink, 1996). One of the two genes responsible for the high-affinity phosphate transport system at the plasma membrane (*PHO89*) is also up-regulated by high-calcium stress in a Crz1-dependent manner (Yoshimoto *et al.*, 2002). This may reflect a relationship between Ca^{2+} and phosphate influx, consistent with the fact that most of vacuolar Ca^{2+} complexes with inorganic polyphosphate (Dunn *et al.*, 1994).

The unfolded protein response (UPR) is induced in situations causing ER stress that lead to incorrect protein folding or to protein traffic overloading at the lumen of this compartment (Walter and Ron, 2011). The response involves the induction of ER/Golgi-associated chaperones and the ERAD machinery for degradation of misfolded proteins. The UPR mediators are evolutionary conserved, and in yeast cells, they include the signaling protein kinase Ire1 and the effector transcription factor Hac1. Among the genes induced by the UPR in *S. cerevisiae* (Travers *et al.*, 2000) are *PDI1* (for protein disulfide isomerase) and *ERO1* (for ER oxidase). These two proteins are necessary for oxidative protein folding in the ER. Partial loss-of-function *ero1* mutants are hypersensitive to the reducing agent dithiothreitol (DTT), whereas the thiol oxidant diamide rescues partially the mutated phenotype (Frand and Kaiser, 1998; Pollard *et al.*, 1998). Ca^{2+} deprivation at the ER also activates the UPR in *S. cerevisiae* (Bonilla *et al.*, 2002), supporting the important role of Ca^{2+} for the correct function of the protein secretory machinery. On the other hand, tunicamycin (an inhibitor of protein N-glycosylation that interferes with protein folding and consequently induces the UPR) provokes Ca^{2+} influx through a mechanism that is Ire1 and Hac1 independent, a phenomenon extensible to other conditions causing ER stress (Bonilla *et al.*, 2002). This, together with the fact that the calcineurin-dependent pathway is required for long-term survival to tunicamycin treatment, indicates that the calcineurin pathway and the UPR operate in parallel for cell protection against ER stress.

Glutaredoxins (GRXs) are glutathione-dependent thiol oxidoreductases that regulate cellular redox processes involving protein sulfhydryl groups (Lillig *et al.*, 2008; Herrero *et al.*, 2010). *S. cerevisiae* contains two GRXs—Grx6 and Grx7, which are integral components of ER/Golgi membranes (Izquierdo *et al.*, 2008; Mesecke *et al.*, 2008b). They share extensive sequence homology between them and with the dithiol GRXs. However, Grx6 and Grx7 contain a single Cys residue at the active site. Considering the 1-Cys mechanism of action of GRXs (Lillig *et al.*, 2008), this supports the idea that Grx6/Grx7 have a deglutathionylation function on uncharacterized targets at ER/Golgi organelles. In spite of their sequence similarities and the fact that both of them become up-regulated upon ER stress by tunicamycin (Izquierdo *et al.*, 2008), Grx6 and Grx7 have certain specificities. Thus Grx6 is enriched at the ER, whereas Grx7 localizes preferentially at Golgi (Izquierdo *et al.*, 2008). In addition, expression of the *GRX6* gene is induced by high-calcium and sodium stresses and by oxidative stress in a Crz1-dependent manner, in contrast to *GRX7* expression (Izquierdo *et al.*, 2008). Finally, Grx6, but not Grx7, contains an iron–sulfur cluster ligand (Mesecke *et al.*, 2008a). These differences point to specialized roles of both GRXs at the membranes of the secretory pathway compartments. In the present work, we show that the absence of Grx6 affects both redox homeostasis at the ER luminal space and Ca^{2+} homeostasis, this last alteration probably being a consequence of a deficient function of Ca^{2+} transporters present in ER membranes. Overall our study reveals the importance of GRXs to carry out redox regulatory functions at the lumen of early secretory membrane vesicles in fungal cells.

RESULTS

The calcineurin pathway is constitutively induced in Δ*grx6* cells

To advance in the functional characterization of Grx6/Grx7, we analyzed the transcriptome of a double Δ*grx6*Δ*grx7* mutant. In our study, 26 genes were constitutively induced at least twofold in the mutant compared with wild-type cells, whereas 11 were repressed (Supplemental Table S1). Among the up-regulated genes, those involved in phosphate metabolism (*PHO89*, *PHO5*, *PHM6*, *PHO11*, *PHO3*, *PHO12*) or in protein secretion/compartmentalization (*ATG15*, *ARE1*, *CPR4*, *PER1*) are predominant. We confirmed the transcriptomic results by Northern analysis of some selected genes, using in addition the single Δ*grx6* and Δ*grx7* mutants (Figure 1). The results indicate that up-regulation of two genes involved in phosphate homeostasis (*PHO89* and *PHM6*) is due to the Δ*grx6* mutation, whereas up-regulation of the other genes tested depends on the Δ*grx7* mutation. *PHO89* and *PHO84* code for the two high-affinity phosphate transporters in yeast (Persson *et al.*, 2003; Mouillon and Persson, 2006). Therefore we also tested whether *PHO84* expression was affected in the absence of Grx6 and/or Grx7. However this was not the case (Figure 1).

Expression of *PHO89*, but not that of *PHO84*, is induced by calcium stress in a Crz1-dependent manner (Yoshimoto *et al.* 2002; Ruiz *et al.*, 2008). Two other genes induced in the Δ*grx6*Δ*grx7* mutant (*THR4* and *CPR4*) contain CDRE consensus motifs in their promoters. These observations point to alterations in the homeostasis of some ions in the absence of Grx6 and/or Grx7. In consequence, we determined whether expression from a Crz1-dependent promoter was constitutively up-regulated in the absence of the two GRXs by using the pAMS366 (wild-type CDRE promoter) and pAMS364 (mutated CDRE promoter) *lacZ* reporter plasmids. In the absence of Grx6, albeit not of Grx7, the CDRE-containing promoter was up-regulated, and this was dependent on the ability to bind the Crz1 factor (Figure 2A). High Ca^{2+} stress was able to induce expression from the intact CDRE promoter in wild-type and Δ*grx7* mutant cells but did not cause significant additional induction over the high

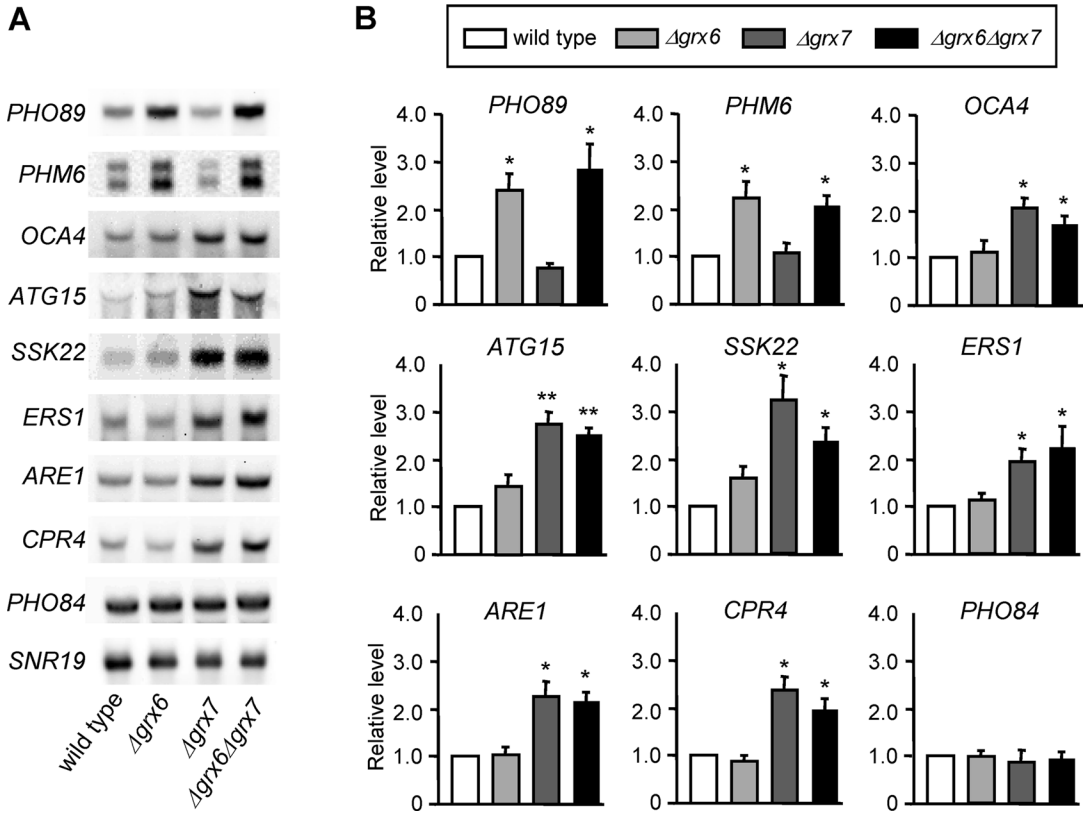

FIGURE 1: Northern blot gene expression analyses in Grx6- and Grx7-deficient strains. (A) Expression of the indicated genes in wild-type (W303-1A), Δ*grx6* (MML890), Δ*grx7* (MML887), and Δ*grx6*Δ*grx7* (MML892) cells growing exponentially in YPD medium. *SNR19* was used as loading control. (B) Quantification of gene expression from Northern blot images. Bars correspond to the mean of three independent experiments ± SD. Values were made relative to the wild-type strain (unit value).

basal constitutive levels in the Δ*grx6* mutant (Figure 2A). By Northern analysis, we confirmed that *CMK2* and *GYP7*, two genes that are up-regulated upon Ca^{2+} stress in a Crz1-dependent manner (Yoshimoto *et al.*, 2002), are also constitutively induced in Δ*grx6* cells and that this induction is abrogated by the Δ*crz1* mutation (Figure 2B).

To confirm that the constitutive induction of the calcineurin pathway in Δ*grx6* cells is biologically significant, we determined the sensitivity of wild-type and mutant cells to the calcineurin inhibitor FK506. The Δ*grx6* and Δ*grx6*Δ*grx7* mutants displayed defective growth in cultures treated with FK506 compared with wild-type or Δ*grx7* cells (Figure 2C). Although the differences were moderate, they were statistically significant. To demonstrate that the growth defects were due to the absence of the enzymatic activity of Grx6 and not indirectly caused by the absence of the protein in the null mutant, we measured growth in FK506-treated cells that expressed a Grx6 active-site mutant protein with a Cys136-to-Ser substitution instead of the wild- type form. Compared to cells expressing wild-type Grx6, those expressing the mutated form had the same growth defects as the mutant lacking any form of Grx6 (Figure 2D). Therefore enzymatically active Grx6 is required for protecting yeast cells in conditions in which the calcineurin pathway is inhibited. In accordance with these results, cells expressing the enzymatically inactive Grx6 form displayed up-regulation of the *CMK2* gene similarly to Δ*grx6* cells (Supplemental Figure S1).

Yeast cells lacking Grx6 have altered levels of Ca^{2+} at the cytosol and ER

Taken together, the foregoing observations suggested that the absence of Grx6 causes constitutive calcium stress in the cell and subsequent induction of the calcineurin pathway, possibly by intracellular accumulation of Ca^{2+}. Therefore we measured cytosolic Ca^{2+} concentration using indo-1 as a fluorescent reporter. Ca^{2+} levels were about double in the Δ*grx6* mutant compared with wild-type cells, whereas the Δ*grx7* mutant did not show abnormal accumulation (Figure 3A). The double Δ*grx6*Δ*grx7* mutant behaves like the Δ*grx6* mutant, confirming that the absence of Grx7 does not influence intracellular calcium homeostasis. Accumulation of Ca^{2+} in Grx6-minus cells was comparable to the accumulation in Δ*pmr1* cells lacking the ER/Golgi SPCA-type pump, and the absence of both Pmr1 and Grx6 has an additive effect in alteration of cytosolic Ca^{2+} (Figure 3A). As reported in earlier studies, in the absence of the P-type pump Spf1 alone, no alteration of Ca^{2+} levels occurs (Cronin *et al.*, 2002), and elimination of Spf1 in a Δ*grx6* mutant did not cause additive effects. Similarly, elimination of the Ca^{2+} exchanger Gdt1 in Δ*grx6* cells had no additional effect on Ca^{2+} accumulation (Figure 3A). In summary, the absence of Grx6 causes accumulation of Ca^{2+}at the cytosol similar to (but independently of) the absence of the Pmr1 pump. To confirm that the activity of Grx6 is responsible for the foregoing phenotype, we determined Ca^{2+} levels in cells that expressed the Grx6 C136S active-site mutant instead of the Grx6 wild-type form. This mutant accumulated Ca^{2+} at similar levels as the Δ*grx6*-null mutant (Figure 3B), confirming that full activity of Grx6 is required for the homeostasis of this ion.

To discriminate between the cytosolic Ca^{2+} pool and that localized in other organelles, we also made determinations after disrupting membranes with DEAE-dextran, which therefore would correspond to total intracellular Ca^{2+}(see *Materials and Methods*). The DEAE-dextran treatment increased significantly the differences in Ca^{2+} levels

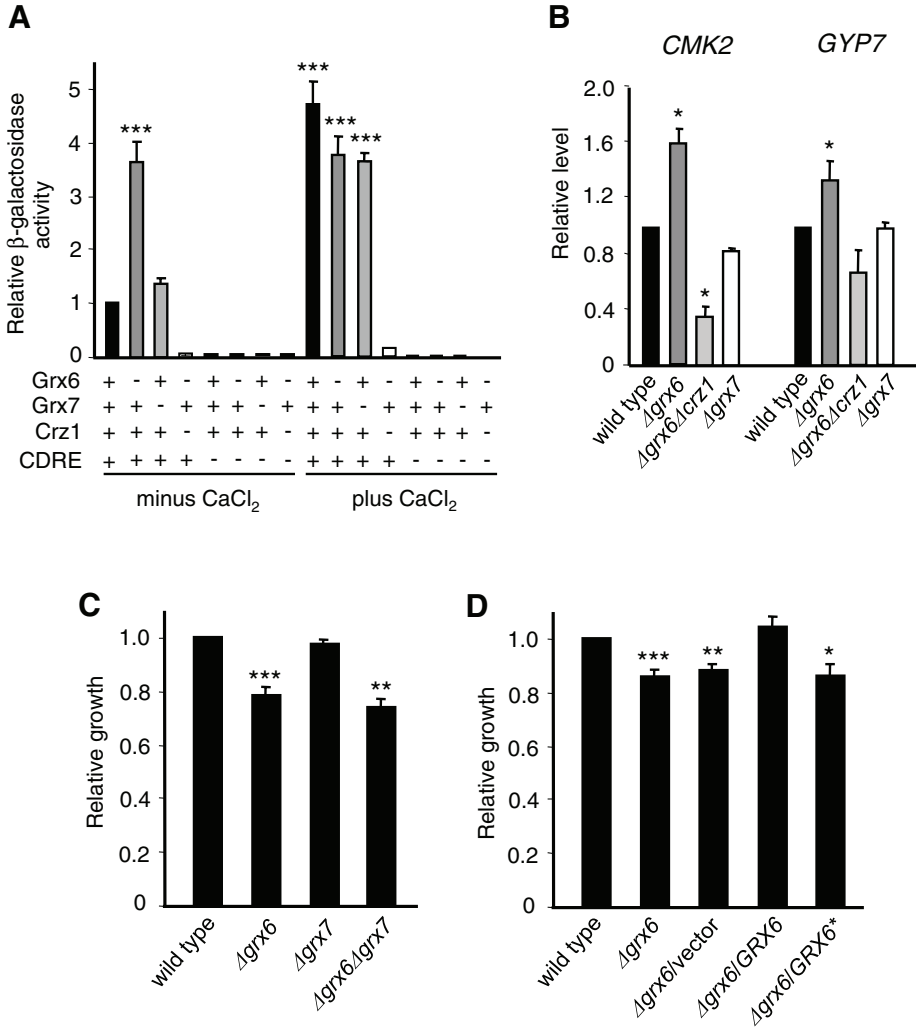

FIGURE 2: Calcineurin pathway–dependent gene expression in Grx6- and Grx7-deficient strains. (A) Wild-type (W303-1A), Δ*grx6* (MML842), Δ*grx7* (MML887), and Δ*grx6*Δ*crz1* (MML1723) cells were transformed with the *lacZ* reporter plasmid pAMS366, which contains functional (+) CDRE motifs, or with plasmid pAMS364, which contains nonfunctional (–) CDRE motifs. Cultures of transformants were exponentially grown in SC medium without or with added (0.2 M, 60 min) $CaCl_2$. β-Galactosidase activity was determined in three independent experiments. Bars indicate the mean ± SD, made relative to the unit value corresponding to pAMS366 transformed with type cells from SC medium without added $CaCl_2$. These conditions were used as reference for statistical analyses. (B) Quantification of the expression of the indicated genes from Northern blot analyses from exponential cultures in YPD medium of the same nontransformed strains indicated in A. Expression of each gene was normalized by the loading control (*SNR19*) and then compared with the respective expression in wild-type cells, which was given the unit value. Bars correspond to the mean of three independent experiments ± SD. (C) Effect of treatment with FK506 (2.5 μg/ml) of the following strains in YPD medium (20 h): wild type (W303-1A), Δ*grx6* (MML890), Δ*grx7* (MML887), and Δ*grx6*Δ*grx7* (MML892). Bars correspond to the mean of at least five independent experiments ± SD, representing the growth yield ratio between treated and untreated cultures for each strain and then made relative to this ratio in wild-type cells. (D) As in C, with the wild-type strain or the Δ*grx6* mutant nontransformed or transformed with the integrative plasmid YIplac128 (vector), pMM1073 (*GRX6*), or pMM1071 (*GRX6**, coding for the C136S mutant form).

between the Δ*pmr1* mutant and wild-type cells compared with the results with nonpermeabilized samples (Figure 3C). This observation is in accordance with the reported Ca^{2+} hyperaccumulation in the vacuoles of Δ*pmr1* cells (Halachmi and Eilam, 1996). On the contrary, membrane permeabilization increased only very moderately the differences between the Δ*grx6* mutant and wild-type cells (Figure 3C), indicating that Ca^{2+} accumulation in this mutant occurs mainly at the cytosol. As expected, the double Δ*grx6*Δ*pmr1* mutant displayed additive accumulation of total intracellular Ca^{2+}. In summary, our results indicate that intracellular Ca^{2+} pools are differentially affected in the absence of Grx6 or Pmr1.

PMC1 expression is also a marker of Ca^{2+} accumulation. In accordance with the foregoing results on Ca^{2+} levels in the mutants, Δ*grx6* and Δ*pmr1* cells expressed higher *PMC1* mRNA levels than wild-type cells, and this increase was additive in the double mutant (Figure 3D).

Next we determined the origin of the excess of Ca^{2+} in Δ*grx6* cells. To this end, we obtained mutants that in addition to Grx6 alternatively lacked Cch1 (subunit of the plasma membrane HACS Ca^{2+} influx machinery), Yvc1 (vacuolar membrane channel for Ca^{2+} release to the cytosol), or Csg2 (ER membrane Ca^{2+} channel). Only the Δ*cch1* mutation suppressed the accumulation of Ca^{2+} in Δ*grx6* cells (Figure 3E), indicating that the excess of this cation results from influx of external sources through HACS rather than from net mobilization of internal organelle stores.

To determine whether cytosolic Ca^{2+} accumulation in Δ*grx6* cells correlated with changes in concentration of the cation at the ER, we used an assay with an ER lumen–targeted aequorin form (Strayle *et al.*, 1999). Results showed that basal ER Ca^{2+} levels were markedly reduced in the Δ*pmr1* mutant compared with wild-type cells, and the response upon Ca^{2+} refilling was also less intense (Figure 3F). The Δ*grx6* cells displayed a pattern similar to the Δ*pmr1* strain, indicating that Ca^{2+} internalization at the ER lumen is compromised in the absence of Grx6. Elimination of Grx6 in cells lacking Pmr1 further accentuated the defects in ER Ca^{2+} accumulation (Figure 3F), confirming the role of this GRX in such process.

The absence of Grx6 causes altered sensitivity to depletion or excess of Ca^{2+}

Other *S. cerevisiae* mutants defective in regulation of intracellular calcium homeostasis display alterations in the sensitivity to Ca^{2+} chelators (reviewed in Cunningham, 2011). Consequently, we tested the sensitivity of Δ*grx6* cells to ethylene glycol tetraacetic acid (EGTA), which chelates extracellular Ca^{2+} ions. In solid medium, the mutant was moderately less sensitive to EGTA than were wild-type cells (Figure 4A). We also quantified the effect of the chelator in liquid medium (Figure 4B), confirming that the Δ*grx6* and the Δ*grx6*Δ*grx7* mutants are less sensitive than wild-type cells in EGTA-treated cultures. Such growth differences were statistically significant and not observed in Δ*grx7* cells. The lower sensitivity of the Δ*grx6* mutant is abrogated by introduction of a Δ*cch1* mutation. These results suggest that previous

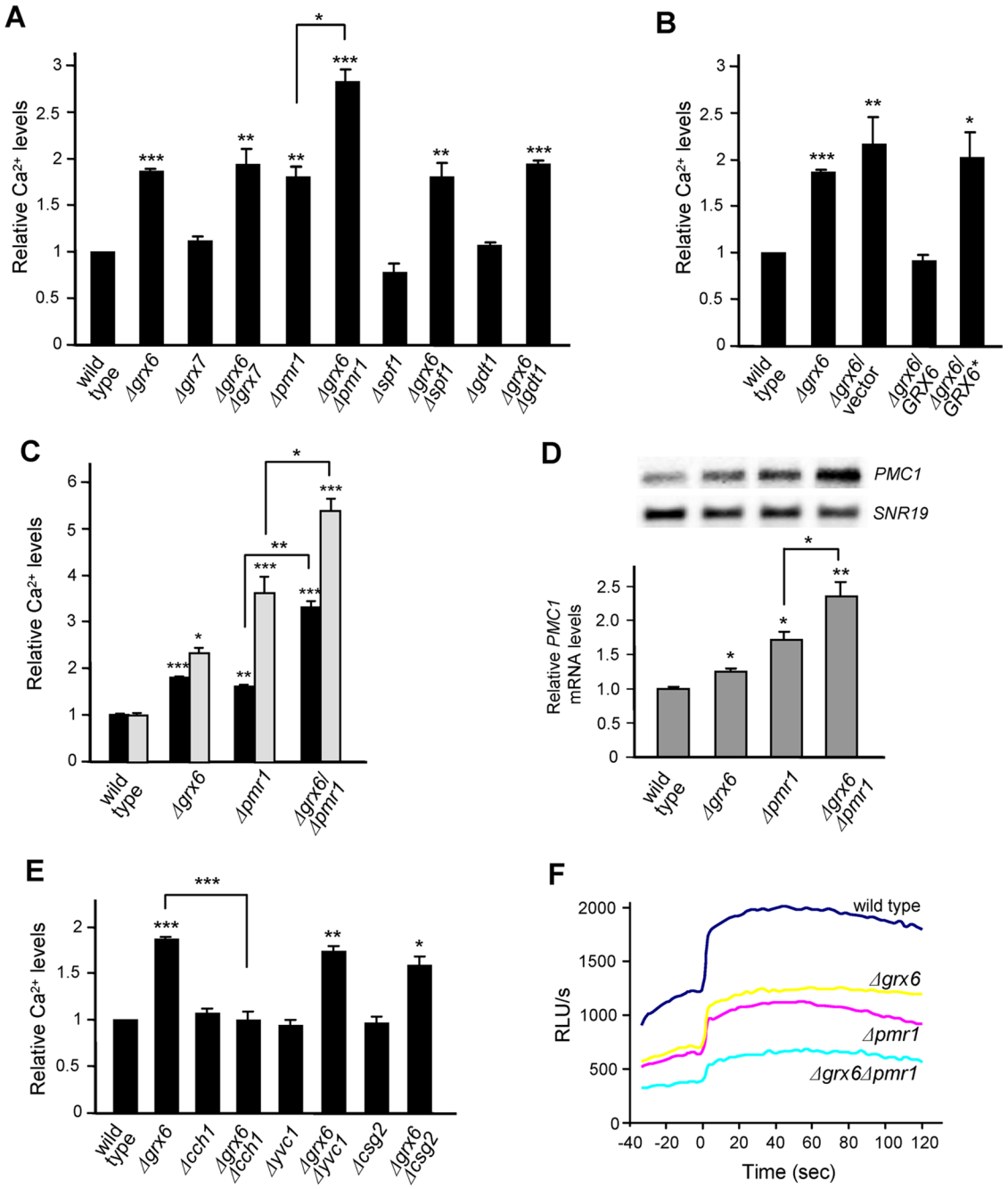

FIGURE 3: Ca^{2+} levels are altered in Grx6-deficient strains. Analyses were done in exponential cultures in YPD medium. (A) Relative cytosolic Ca^{2+} levels, determined by the indo-1 method, in wild type (W303-1A), Δ*grx6* (MML890), Δ*grx7* (MML887), Δ*grx6*Δ*grx7* (MML892), Δ*pmr1* (MML1530), Δ*grx6*Δ*pmr1* (MML1535), Δ*spf1* (MML1716), Δ*grx6*Δ*spf1* (MML1703), Δ*gdt1* (MML1884), and Δ*grx6*Δ*gdt1* (MML1912). The 410/480-nm emission value for each strain (mean of three independent experiments ± SD) was made relative to the wild-type mean value. (B) As in A, with the wild-type strain or the Δ*grx6* mutant nontransformed or transformed with the integrative plasmid YIplac128 (vector), pMM1073 (*GRX6*), or pMM1071 (*GRX6**). (C) Relative Ca^{2+} levels in cytosolic (black bars) or total intracellular (gray bars) fractions. Normalization as in A. For statistical analyses, values were compared with those of the respective compartment in wild-type cells. (D) Northern blot analysis of *PMC1* mRNA in the indicated strains with *SNR19* mRNA as loading control. Quantification of *PMC1* mRNA levels in samples from three independent experiments (mean ± SD), once normalized by *SNR19* mRNA levels and compared with expression in wild-type cells (unit value). (E) As in A, with the following strains: wild type, Δ*grx6*, Δ*cch1* (MML1527), Δ*grx6*Δ*cch1* (MML1548), Δ*yvc1* (MML1526), Δ*grx6*Δ*yvc1* (MML1531), Δ*csg2* (MML1529), and Δ*grx6*Δ*csg2* (MML1538). (F) Relative ER Ca^{2+} levels, represented as luminescence units/s, before and after 1 mM Ca^{2+} reflux (time 0) in cells of the following strains carrying the *STT3::3xHA::AEQ1::LEU2* cassette: wild type (MML1975), Δ*grx6* (MML1977), Δ*pmr1* (MML1979), and Δ*grx6*Δ*pmr1* (MML1981). Represented values are the mean of at least three independent experiments, with three parallel kinetics per experiment. RLU/s_{max} values for each strain (obtained upon final detergent permeabilization and 10 mM $CaCl_2$ treatment; see *Materials and Methods*) were the following: 12,320 (wild type), 11,970 (Δ*grx6*), 11,210 (Δ*pmr1*), and 10,160 (Δ*grx6*Δ*pmr1*).

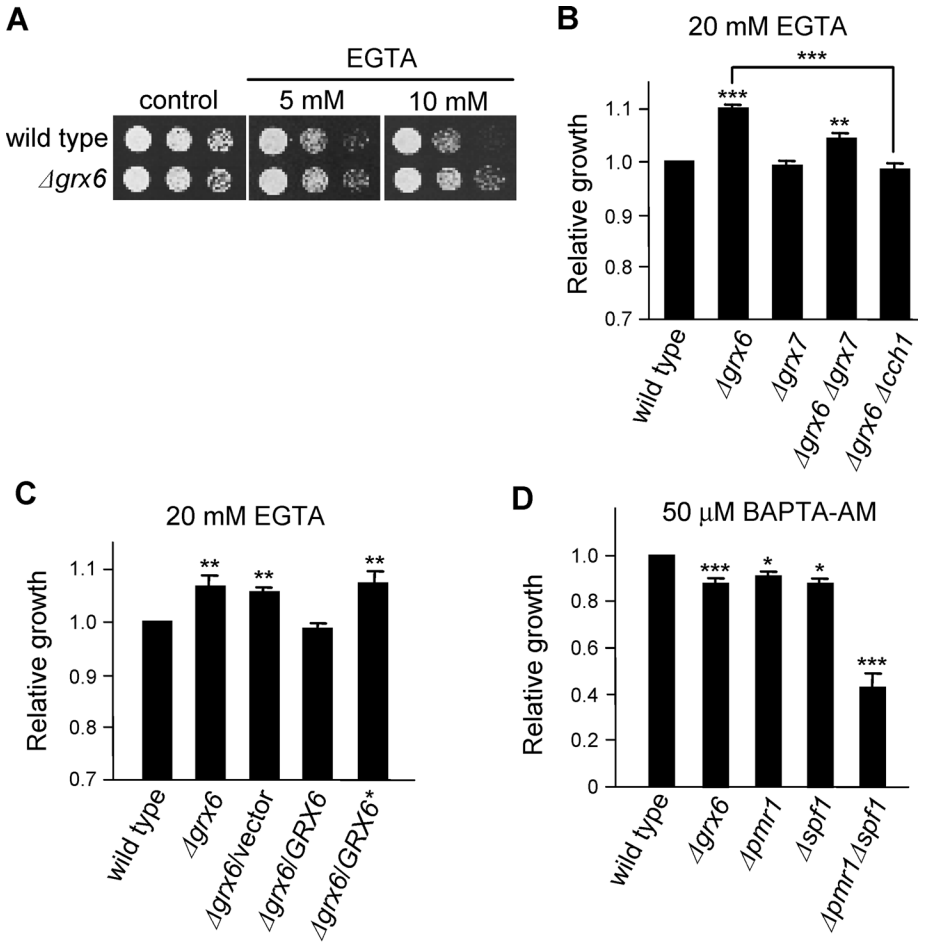

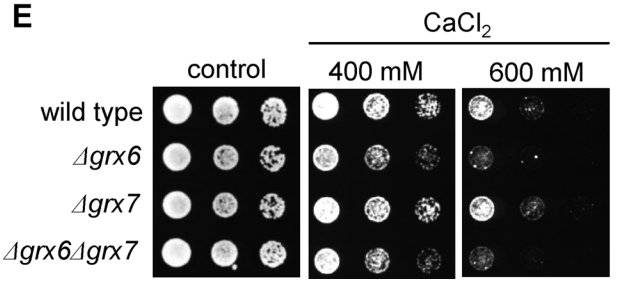

FIGURE 4: Ca^{2+} chelating agents and Ca^{2+} excess affect growth of Grx6-deficient strains. (A) Sensitivity of wild-type (W303-1A) and Δ*grx6* (MML890) cells to EGTA. Serial dilutions (1:5) of the respective exponential cultures were spotted on YPD plates with the indicated concentrations of the agent. Growth was recorded after 2 d at 30°C. (B) Effect of treatment with EGTA (20 h) of the following strains in YPD liquid medium: wild type (W303-1A), Δ*grx6* (MML890), Δ*grx7* (MML887), Δ*grx6*Δ*grx7* (MML892), and Δ*grx6*Δ*cch1* (MML1548). Bars correspond to the mean of at least five independent experiments ± SD, representing the growth yield ratio between treated and untreated cultures for each strain and then made relative to this ratio in wild-type cells. (C) As in B, with the wild-type strain or the Δ*grx6* mutant nontransformed or transformed with the integrative plasmid YIplac128 (vector), pMM1073 (*GRX6*), or pMM1071 (*GRX6**). (D) Effect of treatment with BAPTA-AM (20 h) of the following strains in YPD liquid medium: wild type (W303-1A), Δ*grx6* (MML890), Δ*pmr1* (MML1530), Δ*spf1* (MML1716), and Δ*pmr1*Δ*spf1* (MML1710). Bars correspond to the mean of at least five independent experiments ± SD, normalized as in B. (E) Sensitivity of wild-type, Δ*grx6*, Δ*grx7*, and Δ*grx6*Δ*grx7* cells to the indicated concentrations of $CaCl_2$. Growth on modified SD solid medium was recorded after 4 d at 30°C.

overaccumulation of intracellular calcium protects the mutant cells against the calcium starvation effects caused by EGTA. The Grx6 C136S mutant has the same sensitivity phenotype to EGTA as the null Δ*grx6* mutant (Figure 4C), again confirming that these effects are caused by the lack of thiol oxidoreductase activity in the mutated Grx6 molecule.

Whereas EGTA chelates extracellular calcium, BAPTA-AM is membrane permeable and is therefore able to chelate intracellular Ca^{2+} in yeast cells (Li *et al.*, 2011). In contrast to EGTA, the Δ*grx6* mutant was moderately (although significantly) more sensitive to BAPTA-AM than were wild-type cells (Figure 4D). The ER membrane Ca^{2+} transporter mutants Δ*pmr1* and Δ*spf1* also displayed increased sensitivity to BAPTA-AM, and this was especially manifested in the double Δ*pmr1*Δ*spf1* mutant, consistent with the overlapping role of both transporters in regulating Ca^{2+} content in the ER lumen (Cronin *et al.*, 2002).

Other yeast mutants in intracellular Ca^{2+} compartmentalization, in addition to being hypersensitive to chelators of the cation, also display high sensitivity to calcium excess. In accordance with the observed alterations in Ca^{2+} accumulation, the Δ*grx6* mutation provoked moderate hypersensitivity to extracellular high Ca^{2+} concentration, in contrast to the Δ*grx7* mutation (Figure 4E).

The Δ*grx6* mutant also overaccumulates intracellular phosphate

Given the relationship between calcium and phosphate homeostasis in yeast cells, we measured intracellular orthophosphate levels in the Δ*grx6* and Δ*grx7* mutants. The Δ*grx6* cells accumulate twice as much intracellular orthophosphate as wild-type and Δ*grx7* mutant cells (Figure 5A). The abnormal accumulation of orthophosphate in Δ*grx6* cells is totally rescued by deletion of the *PHO89* gene, whereas introduction of the Δ*grx6* mutation in cells lacking the other high-affinity phosphate transporter, Pho84, still causes higher orthophosphate levels compared with those in the single Δ*pho84* mutant (Figure 5A), pointing to Pho89 as the main agent responsible for the accumulation of orthophosphate in the absence of Grx6. We next determined where this excess of phosphate became accumulated in the Δ*grx6* cells. Vacuoles were isolated from cytosolic and other membranous compartments by centrifugation in a Ficoll gradient, and a vacuolar fraction was isolated that was not detectably contaminated by cytosolic or mitochondrial proteins (Figure 5B). A fraction enriched in cytosolic proteins but contaminated by vacuolar proteins was considered as cytosolic fraction. Orthophosphate and polyphosphate levels were measured separately in both fractions, and the results showed that both forms of phosphate become accumulated in the cytosolic fraction of the Δ*grx6* cells compared with the wild type, whereas the vacuolar fraction of the mutant cells exhibits reduced levels of both

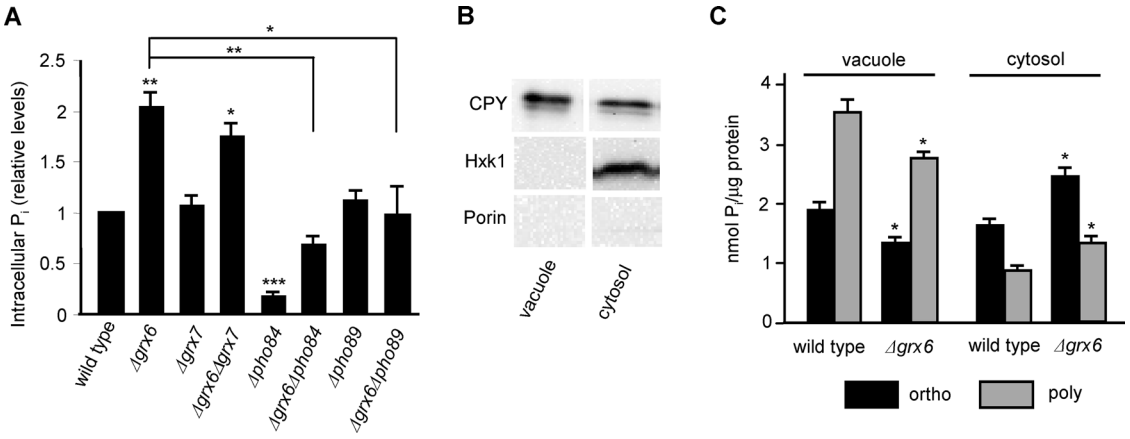

FIGURE 5: Grx6-deficient cells accumulate phosphate intracellularly. (A) Orthophosphate levels in cells (growing exponentially in YPD medium) of the following strains: wild type (W303-1A), Δ*grx6* (MML890), Δ*grx7* (MML887), Δ*grx6*Δ*grx7* (MML892), Δ*pho84* (MML1304), Δ*grx6*Δ*pho84* (MML1337), Δ*pho89* (MML1306), and Δ*grx6*Δ*pho84* (MML1313). Values (mean of three independent experiments ± SD) are made relative to wild-type cells. (B) Purity of vacuolar and cytosolic cell fractions from wild-type cells growing exponentially in YPD medium, tested by Western blot with antibodies against CPY (vacuolar marker), Hxk1 (cytosolic marker), and porin (mitochondrial marker). (C) Orthophosphate and polyphosphate content in purified vacuolar and cytosolic fractions from wild-type and Δ*grx6* cells growing exponentially in YPD medium. For statistical analyses, values in the mutant were compared with those of the respective compartment in wild-type cells.

orthophosphate and polyphosphate (Figure 5C). Therefore compartmentalization of phosphate is altered in the absence of Grx6, resulting in a significant accumulation at the cytosol.

The absence of Grx6 counteracts defects in the ER protein folding machinery

The UPR is not constitutively induced in the Δ*grx6* mutant (Izquierdo *et al.*, 2008). However, we explored whether the lack of Grx6 could exacerbate the UPR in the presence of agents that by themselves interfere with the protein-folding machinery. To analyze it, we used *ERO1* and *PDI1* expression as reporter of the activation of the UPR (Yoshimoto *et al.*, 2002). As expected, the protein-reductant DTT activated the UPR in wild-type cells in a transient way, but this activation was more intense in Δ*grx6* cells (Figure 6A). This is in contrast with Δ*grx7* cells, which displayed even a milder response than wild-type cells. The increased induction of the UPR upon interference with the protein-folding machinery in the absence of Grx6 could point to a relationship of the latter with this machinery.

The UPR target Ero1 is an essential ER oxidase required for appropriate protein folding (Frand and Kaiser, 1998; Pollard *et al.*, 1998). To determine the possible genetic interactions between *ERO1* and *GRX6*, we constructed a mutant in which the endogenous *ERO1* promoter was substituted by the doxycycline-regulatable $tetO_2$ promoter (Bellí *et al.*, 1998a), and we introduced the Δ*grx6* mutation in that strain. As expected, the wild-type strain for *GRX6* that expressed *ERO1* under the $tetO_2$ promoter did not grow after switching off this promoter. As occurs with the conditional temperature-sensitive *ero1-1* mutation (Frand and Kaiser, 1998), the thiol oxidant diamide abolished the growth defects caused by down-regulation of *ERO1* expression in the conditional $tetO_2$-*ERO1* strain at 36ºC (Figure 6B), although not at 30ºC (unpublished data). The diamide ability to compensate for the absence of Ero1 activity seems therefore to be temperature dependent. Introduction of the Δ*grx6* mutation rescued partially, although significantly, the lethality due to the absence of *ERO1* expression (Figure 6B). These results therefore support a role for Grx6 in the redox conditions of the ER, which would become more oxidized in its absence. This in turn would compensate for the absence of the Ero1 oxidase.

We showed (Izquierdo *et al.*, 2008) that lack of Grx6 and/or Grx7 in an otherwise wild-type genetic background does not affect the pool of mature carboxypeptidase Y (CPY), a vacuolar protein that is processed during secretion along ER/Golgi compartments and is used as a reporter for the functionality of the secretory machinery. In accordance with those results, in pulse and chase experiments, conversion of the precursor to the mature form of CPY followed the same kinetics in Δ*grx6* and Δ*grx7* cells as in wild-type cells (Figure 7A). Given the aforementioned interaction of Grx6 with Ero1 and the UPR, we analyzed CPY maturation kinetics in the Δ*grx6* mutant under doxycycline-regulated conditional expression of *ERO1*. As expected from other work (Frand and Kaiser, 1998; Pollard *et al.*, 1998), a significant delay in CPY maturation was observed when Ero1 function was compromised compared with the control conditions without doxycycline (Figure 7B). This was especially evident just after the pulse period (0 min), in which almost all newly synthesized CPY remained in the precursor form when Ero1 levels were depleted. However, introduction of the Δ*grx6* mutation rescued the defects in CPY processing in these same Ero1-deficient conditions, as happens after diamide addition (Figure 7B). These results paralleled those on cell growth (Figure 6B) and supported the notion that the oxidant conditions created in the absence of Grx6 partially restore the previously compromised functionality of the protein folding/secretion machinery due to low Ero1 levels. To confirm this, we made real-time measurements of the redox state of the ER lumen in the foregoing strains and conditions, using a redox-sensitive ero–green fluorescent protein (GFP) form oriented to the ER lumen (Merksamer *et al.*, 2008). Constitutive oxidizing conditions at the ER lumen and the subsequent reductive response upon DTT application were similar in *GRX6* and Δ*grx6* cells expressing Ero1, with slow recovery to basal conditions after application of the reductive stress (Figure 7C). In contrast, Ero1-deficient conditions constitutively created a moderate overoxidized state at the ER that was much exacerbated in cells lacking Grx6. In addition, the latter cells rapidly returned to the overoxidized conditions upon DTT treatment (Figure 7C). We can conclude that the absence of Grx6 causes overoxidation of the pool of cysteine sulfhydryls at the ER lumen, as becomes clearly manifested in Ero1-deficient cells.

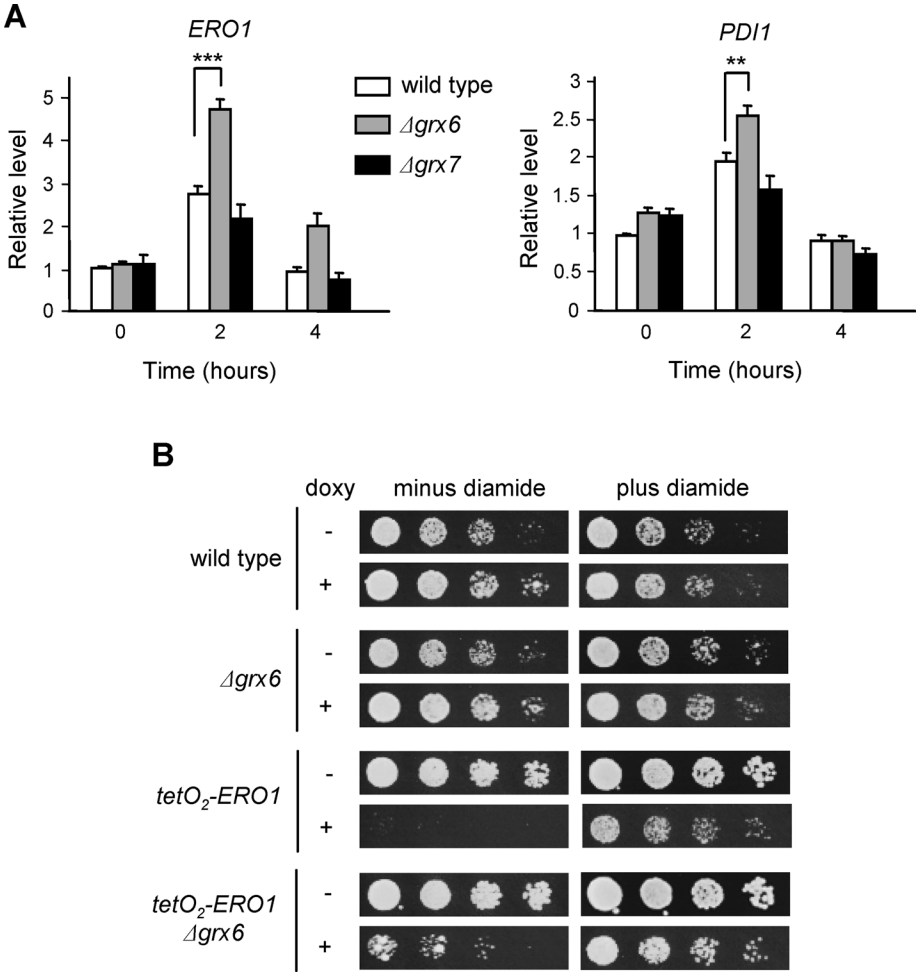

FIGURE 6: Grx6 interacts functionally with UPR components. (A) Quantification of expression of the indicated genes from Northern blot analyses. Samples were obtained from exponential cultures in YPD medium of wild-type (W303-1A), Δ*grx6* (MML890), and Δ*grx7* (MML887) cells that were treated for the indicated times with DTT (2 mM). Expression of each gene was normalized by the loading control (*SNR19* mRNA) and then compared with the respective expression in wild-type cells, which was given the unit value. Bars correspond to the mean of three independent experiments ± SD. (B) Cultures of wild-type (W303-1A), Δ*grx6* (MML890), *tetO*$_2$*-ERO1* (MML1221), and *tetO*$_2$*-ERO1*Δ*grx6* (MML1789) cells in SC medium at 25°C were serially diluted (1:5) and spotted on SC medium plates without or with doxycycline (2 µg/ml) and without or with diamide (0.3 mM). Growth was recorded after 3 d of incubation at 36°C.

Phenotypic alterations in Ca^{2+} homeostasis and protein secretion in Grx6-minus cells can be rescued independently

The Ca^{2+} homeostasis defects in Δ*grx6* cells are observed in conditions in which alterations in the protein secretion machinery are not apparent, at least for CPY (Figure 7A). To support this observation, we measured intracellular Ca^{2+} levels in Ero1-deficient cells with diamide, which display wild-type–like CPY processing. In these conditions, the Δ*grx6* mutation still provoked increased accumulation of intracellular Ca^{2+} (Figure 8A), confirming that this accumulation occurs independently of the functionality of the ER protein-folding machinery. We also studied whether reducing cytosolic Ca^{2+} levels (by introducing a Δ*cch1* mutation) in Grx6-minus Ero1-deficient cells interfered with the ability to rescue CPY processing. In fact, the *tetO*$_2$*-ERO1*Δ*grx6*Δ*cch1* mutant accumulated calcium levels similar to control *GRX6* cells (Figure 8A), but CPY processing still occurred efficiently in doxycycline-treated cells in spite of the low Ero1 levels (Figure 8B). In summary, both phenotypes, respectively related to CPY processing and calcium accumulation in Δ*grx6* cells, can be rescued independently of each other, indicating that one is not a direct consequence of the other. We confirmed that alterations in Ca^{2+} homeostasis are downstream of the general redox function of Grx6 at ER/Golgi by demonstrating that a Δ*pmr1* mutation does not rescue the growth defects of Ero1-deficient cells, in contrast to the Δ*grx6* mutation (Supplemental Figure S2).

The previous results supported the participation of the redox activity of Grx6 in regulation of protein thiols at the ER/Golgi lumen. In this context, accumulation of cytosolic Ca^{2+} could result from disrupting such a regulatory role of Grx6. If this were the case, reductive stress could compensate for the absence of Grx6 and return cytosolic Ca^{2+} to wild-type levels. Our results with DTT-treated cells (Figure 8C) confirm this hypothesis, allowing us to propose a thiol-regulatory role in Ca^{2+} homeostasis for Grx6.

DISCUSSION

Yeast Grx6 and Grx7 are the first non-PDI glutathione-dependent thiol oxidoreductases described as associated to the protein secretory machinery. On the basis of our transcriptome results with the respective mutants, we focused this study on the functional characterization of Grx6. One-cysteine GRXs like Grx6 or Grx7 lack the capacity to reduce protein disulfides. Their enzyme activity consists of deglutathionylating mixed disulfides between glutathione and protein thiols, releasing reduced glutathione (GSH; Lillig *et al.*, 2008; Deponte, 2013). Protein glutathionylation is a reversible mechanism for protecting protein thiols against irreversible oxidative modifications, in addition to having signaling functions (Gallogly and Mieyal, 2007). Such a protective role may be of great importance in the oxidant environment of the early secretory vesicles. In addition, the equilibrium between glutathionylated and deglutathionylated protein forms at the ER may be a mechanism to regulate the redox ratio between free GSH and oxidized glutathione. The latter may exist as dimers (GSSG) or by forming mixed disulfides with proteins. Because GSH is important for the activity of the Ero1/PDI machinery (Cuozzo and Kaiser, 1999; Chakravarthi *et al.*, 2006; Sevier and Kaiser, 2008), ER/Golgi GRXs could act as general regulators of protein folding through their oxidoreductase activity on glutathione–protein mixed disulfides. In fact, the role of GRXs as facilitators of protein folding was proposed earlier (Berndt *et al.*, 2008).

Using the ero-GFP reporter, we observed that a Δ*grx6* mutant does not display altered redox homeostasis at the ER in the presence of Ero1 function. However, *ERO1* expression down-regulation causes a moderate redox shift toward a higher oxidation state that is much more intense in the absence of Grx6. That is, the lack of this GRX results in a significant oxidation of the ER lumen over basal conditions, provided that Ero1 levels are under normality. In wild-type conditions for *ERO1*, the redox equilibrium due to balanced

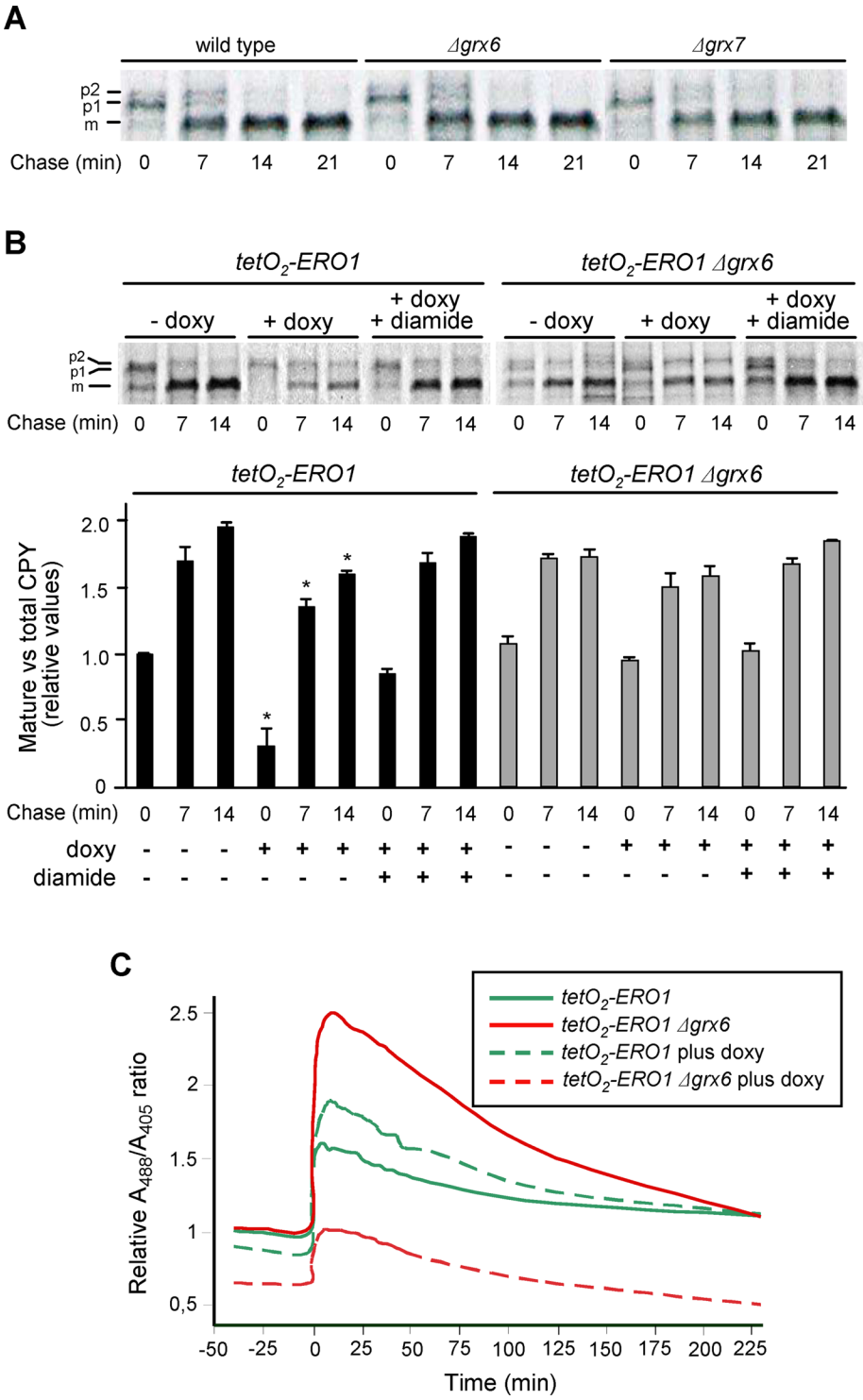

FIGURE 7: Grx6 activity influences the redox state of the ER in Ero1-depleted cells. (A) Exponential cultures in SC medium of wild-type (W303-1A), Δ*grx6* (MML890), and Δ*grx7* (MML887) cells were pulse labeled with [^{35}S]methionine/[^{35}S]cysteine for 6 min and chased for the indicated times. Immunoprecipitated CPY was visualized by autoradiography after SDS–PAGE separation. The position of the ER (p1), Golgi (p2), and mature vacuolar (m) forms of CPY (Vashist *et al.*, 2002) is indicated. (B) Cells of the *tetO$_2$-ERO1* (MML1221) and *tetO$_2$-ERO1*Δ*grx6* (MML1789) strains were grown exponentially at 25°C and then shifted to 36°C. Doxycycline alone (2 μg/ml) or plus diamide (0.3 mM) was added to part of these cultures at the time of the temperature shift, and after 9 h they were pulse labeled for 5 min, chased, and processed as in A. The graphic indicates the fraction of the mature form relative to total CPY after autoradiography signal quantification. Values (mean of three independent experiments) were made relative to those of *tetO$_2$-ERO1* cells at time 0 (unit value). For statistical analyses, for each of the two strains, the values at each chase time in treated cultures (doxycycline and/or diamide) were compared with the respective values at the same chase time in untreated cultures. (C) Cultures of the indicated strains were grown in SC medium at 36°C with doxycycline (9 h, 2 μg/ml) or without the antibiotic. At time 0, DTT (2 mM) was added. The ratio of emission at 488 nm vs. 405 nm (made relative to the value in the samples of *tetO$_2$-ERO1* cells without doxycycline at time 0) is represented.

Ero1/Pdi1 activities (Kim *et al.*, 2012) could compensate for the absence of Grx6 with no significant effect on the GSH/oxidized glutathione ratio. This would not occur in Ero1-depletion conditions. In this situation, the deglutathionylating activity of Grx6 could restore, at least partially, the redox equilibrium by releasing GSH from the mixed disulfides. The overoxidation state created by the absence of Grx6 in Ero1-depletion conditions would be comparable to that created by the oxidant diamide in a thermosensitive *ero1-1* mutant (Frand and Kaiser, 1998), with similar implications concerning rescue of Ero1 functional defects in relation to CPY secretion/maturation and general cell growth. These results support a role for the disulfide reductant activity of Grx6 in modulating the glutathionylation state of target proteins at the ER/Golgi lumen and consequent regulation of the glutathione redox balance. GRXs act as thiol reductants or oxidants, depending on the redox state of the enzyme environment (Lillig *et al.*, 2008). The observations on Grx6-minus cells provide evidence that this GRX has a reductant activity in spite of the highly oxidant environment of the ER lumen.

Under normal Ero1 levels, secretion of the CPY reporter is not altered in a Δ*grx6* mutant. However, the fact that some effects on the protein-folding machinery still occur in these conditions is supported by the more intense up-regulation of the UPR in the mutant upon treatment with protein-unfolding agents. Perhaps in Δ*grx6* cells, partial depletion of GSH at the ER lumen due to the absence of the deglutathionylating activity of Grx6 would result in intrinsic defects in the folding machinery, given the requirement of GSH for Ero1 activity (Cuozzo and Kaiser, 1999). These defects would become phenotypically manifested only upon treatment with external agents further compromising protein folding. Remarkably, such UPR up-regulation is not similarly observed in a Δ*grx7* mutant, maybe due to a more secondary role of Grx7 in redox regulation of the vesicles lumen or

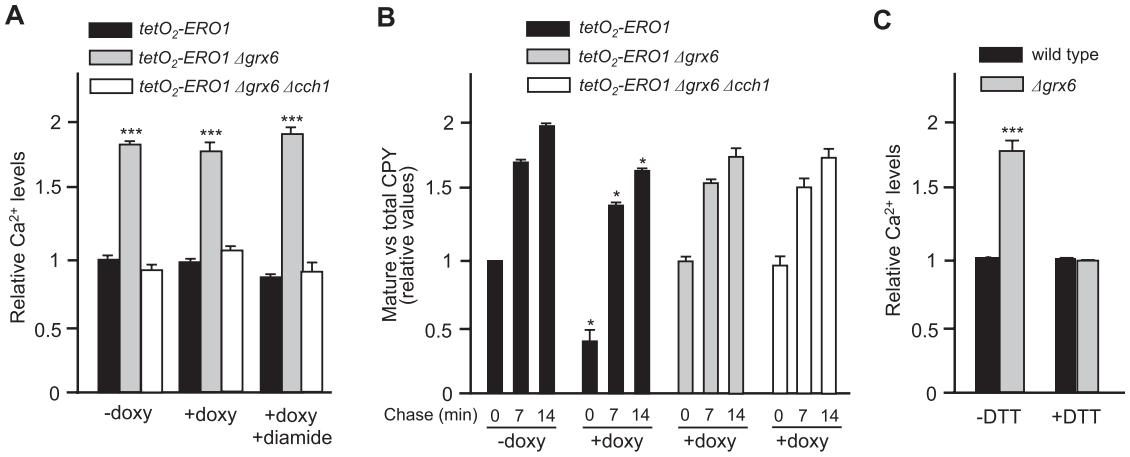

FIGURE 8: Alteration of intracellular Ca^{2+} levels in the absence of Grx6 can be dissected experimentally from alterations in CPY processing. (A) Relative cytosolic Ca^{2+} levels, determined by the indo-1 method, in *tetO$_2$-ERO1* (MML1221), *tetO$_2$-ERO1Δgrx6* (MML1789), and *tetO$_2$-ERO1Δgrx6Δcch1* (MML1965) cells. These were grown exponentially at 25°C in YPD medium and then shifted to 36°C without or with doxycycline (2 μg/ml) and without or with diamide (0.3 mM). Samples were taken after 14 h in these conditions for cytosolic Ca^{2+} determination. The 410/480-nm emission value for each strain and condition (mean of three independent experiments ± SD) was made relative to the mean value of wild-type cells without treatments, and this was taken as reference for statistical analyses. (B) The strains indicated in A were subjected to pulse and chase experiments for quantification of mature versus total CPY. See legend to Figure 7, A and B, for details. For statistical analyses, values at each chase time in doxycycline-treated cultures were compared with the respective values at the same chase time in untreated cultures of *tetO$_2$-ERO1* cells. (C) Relative cytosolic Ca^{2+} levels in wild-type (W303-1A) and Δ*grx6* (MML890) cells growing exponentially in SC medium and then subjected to DTT treatment (2 mM, 3 h). The 410/480-nm emission values (mean of three independent experiments ± SD) are made relative to the untreated wild-type cells.

alternatively to the fact that Grx7 seems to have an exclusive location at Golgi, whereas UPR signaling occurs at the ER.

Although not contradicting a possible general regulatory role of ER/Golgi GRXs on the GSH/oxidized glutathione ratio at the vesicles lumen, Grx6 may have specific protein targets, as its absence results in specific phenotypes not shared with the Δ*grx7* mutant. Thus we demonstrated that the Δ*grx6* mutant (but not Δ*grx7* cells) has higher than normal cytosolic Ca^{2+} levels, and that the mutant cells incorporate the cation from external sources. In contrast, the mutant is deficient in Ca^{2+} accumulation at the ER lumen. It is noteworthy that this depletion of Ca^{2+} at the ER lumen does not cause constitutive activation of the UPR, similar to what occurs in Δ*pmr1* cells (Durr *et al.*, 1998). The alteration in Ca^{2+}distribution occurs in Δ*grx6* cells in conditions in which CPY maturation is apparently not affected, that is, in cells with normal Ero1/PDI functions, as well as in diamide-treated Ero1-depleted cells otherwise lacking Grx6 function. These results point to a specific redox function of Grx6 on some regulator of Ca^{2+} homeostasis inside the cell. We propose that this regulator would be a Ca^{2+} transporter whose activity would be modulated through the deglutathionylation activity of Grx6. In support of this hypothesis, treatment of Δ*grx6* cells with the thiol reductant DTT reduces Ca^{2+} levels in the mutant to wild-type ones. The accompanying overaccumulation of phosphate inside Δ*grx6* cells would be consequence of the activation of the calcineurin pathway in this mutant, one of its targets being *PHO89*, which encodes for one of the two high-affinity phosphate transporters at the yeast plasma membrane. In fact, our results indicate that Pho89 is the main agent responsible for the observed phosphate accumulation. Phosphate acts as a buffer in yeast cells for regulating the excess of free calcium and other cations (Dunn *et al.*, 1994; Eide *et al.*, 2005).

In mammalian cells, functional redox regulation has been demonstrated for several ER Ca^{2+} transporters, among them the SERCA pumps and the cardiac Ca^{2+} release channels (also known as ryanodine receptors; Zima and Blatter, 2006; Raturi *et al.*, 2014). SERCA 2b activity is regulated by ERp57, a multifunctional ER thiol oxidoreductase member of the PDI family (Li and Camacho, 2004; Turano *et al.*, 2011). About the redox-regulated target of Grx6, given its ER/Golgi location, attention should be initially focused on the Ca^{2+} transporters in these organelles: the Pmr1 and Spf1 pumps, the Gdt1 exchanger, and the Csg2 channel. Pmr1 is the main controller of intra-ER/Golgi Ca^{2+} necessary among other functions for manosylation of secretory proteins (Cunningham, 2011). In case Grx6-mediated deglutathionylation of Pmr1 were required for activation of the pump, this would result in lack of Pmr1 function in Δ*grx6* cells. However, this is not compatible with some of the observed phenotypes in the respective single and double mutants. Thus 1) Δ*pmr1* cells accumulate Ca^{2+} preferentially at the vacuole (through activation of the calcineurin-dependent pathway and consequent up-regulation of *PMC1*), whereas in Δ*grx6* cells, Ca^{2+} accumulation occurs at the cytosol; 2) Δ*pmr1* cells display retarded CPY maturation/secretion (Vashist *et al.*, 2002), in contrast to the Δ*grx6* mutant; and 3) cytosolic accumulation of Ca^{2+} and depletion at the ER are additive between the Δ*pmr1* and Δ*grx6* mutations, definitively pointing to independent roles for both proteins. A scenario in which Pmr1 deglutathionylation by Grx6 would result in its inhibition would also be incompatible with the foregoing phenotypes.

The fact that the Δ*grx6*Δ*spf1* mutant accumulates intracellular Ca^{2+} to the same levels as the single Δ*grx6* mutant and in contrast to the single Δ*spf1* mutant (Cronin *et al.*, 2002; this study) argues against Grx6 as a direct regulator of Spf1, either as activator (in which case, both single mutants would have similar phenotypes) or deactivator (which would result in similar phenotypes for Δ*spf1* and Δ*grx6*Δ*spf1* cells). Similar arguments apply for Grx6 as potential regulator of the Ca^{2+} exchanger, Gdt1. In summary, not Pmr1, Spf1, or Gdt1 appears to be a direct redox target of Grx6, as least when separately considered. Another possible interpretation would result

from considering compensatory effects of the absence of some of them on the activity of the remaining transporters in order to maintain robust control of Ca^{2+} homeostasis or alternatively by considering the existence of an intermediate regulation level between Grx6 and Ca^{2+} entry at the ER. The primary role of Csg2 as a channel exporting Ca^{2+} from the ER to the cytosol is more controversial, as it has also been characterized as a Ca^{2+}-binding protein involved in the synthesis of sphingolipids (Zhao *et al*., 1994). The absence of Csg2 does not provoke intracellular Ca^{2+} accumulation (Tanida *et al*., 1996; this study) and does not suppress the cytosolic accumulation of the cation in Δ*grx6* cells, eliminating a direct regulatory function of Grx6 on Csg2 as the explanation for the observed phenotype of the mutants. The possibility is open that other, still-unknown proteins involved in Ca^{2+} movement to or from the cytosol exist that could be the direct targets of Grx6 redox activity. We cannot discard Mid1 (one of the three components of the plasma membrane HACS complex) as a possible Grx6 target. In fact, Mid1 has been reported to localize also at the ER (Yoshimura *et al*., 2004), and it contains a cysteine-rich domain (similar to the α2δ subunits of mammalian voltage-gated Ca^{2+} channels; Martin *et al.,* 2011), which could be implicated in regulation of its activity. This hypothesis would be compatible with reversion of the Δ*grx6* calcium-related phenotypes by abolishing HACS activity in a Δ*cch1* mutant.

GRXs of the Grx6/Grx7 subfamily are present only in fungi. In higher eukaryotes, their function might be carried by PDI family members, as experimentally demonstrated for the SERCA 2b pump. In fact, this family displays larger diversification of functionally specialized members in mammals than in yeast and other fungi (Oka and Bulleid, 2013). In any case, modulation of intracellular Ca^{2+} homeostasis through thiol redox regulation of transporters may be evolutionary conserved in eukaryotes.

MATERIALS AND METHODS

Strains and plasmids

Strains used in this study derive from *S. cerevisiae* wild-type W303 and are listed in Supplemental Table S2.

Plasmids pAMS366 and pAMS364 drive expression of the *lacZ* reporter gene respectively from four wild-type copies in tandem of CDRE or from mutated CDRE forms unable to bind Crz1 (Stathopoulos and Cyert, 1997). Plasmid pJS79 carries a *STT3::3xHA::AEQ1::LEU2* cassette that can be mobilized into the chromosomal *STT3* locus as a *Sph*I–*Spe*I fragment (Strayle *et al*., 1999). It allows expression of a 3HA-aequorin protein with the Ca^{2+}-sensitive site targeted to the ER lumen. Plasmid pMM1071 derives from pMM822 (Izquierdo *et al*., 2008) by mutagenizing the active-site Cys-136 codon of the *GRX6* open reading frame (ORF) into a Ser codon using the ExSite method (Weiner and Costa, 1995), followed by subcloning a *Bam*HI–*Pst*I fragment containing the mutagenized *GRX6* ORF plus promoter and downstream regions into the polylinker of the *LEU2* vector YIplac128 (Gietz and Sugino, 1988). Mutation was confirmed by DNA sequencing. In parallel, pMM1073 was obtained by direct subcloning of the *Bam*HI–*Pst*I fragment of pMM822 containing wild-type *GRX6* plus adjacent sequences into YIplac128. Plasmids were integrated at the *LEU2* locus of the transformed strain after linearization by *Eco*RV digestion.

Growth media and culture conditions

YPD (1% yeast extract, 2% peptone, 2% glucose) or synthetic SC medium (Sherman, 2002) was usually used for *S. cerevisiae* cell growth at a temperature of 30°C unless otherwise indicated. Media were solidified with 2% agar. Plate assays of growth sensitivity were done by spotting serial 1:10 dilutions of exponential cultures onto medium plates containing the corresponding agent and recording growth after 2 or 3 d of incubation at 30°C. For sensitivity to $CaCl_2$ stress, a modified synthetic SD medium was used (Demaegd *et al*. 2013).

Growth in liquid medium of several strains under parallel separate treatments (in 0.5-ml cultures initially inoculated with 2×10^5 cells) was automatically recorded ($OD_{600\ nm}$) at 1-h intervals, using shaken microtiter plates sealed with oxygen-permeable plastic sheets, in a PowerWave XS (BioTek, Winooski, VT) apparatus at controlled temperature. Treatments were applied to cells that had been growing previously during at least 10 generations in exponential conditions. For the tested strains, the ratio of the automatically recorded optical density values (growth yield) between treated and untreated cultures after different time periods was calculated and then made relative to the same ratio in the wild-type strain (unit value).

Genetic methods

Standard protocols were used for DNA manipulations and transformation of yeast cells. Single-null mutants were generated using the short-flanking homology approach after PCR amplification of the *natMX4* or *kanMX4* cassettes and selection for resistance to nourseothricin (Goldstein and McCusker, 1999) or Geneticin (Wach *et al*., 1994), respectively. Disruptions were confirmed by PCR analysis. The endogenous *ERO1* promoter was substituted by the $tetO_2$ promoter using the *kanX4*-based cassette from plasmid pCM224 as described by Bellí *et al*. (1998a). Multiple mutants were obtained by crossing the parental mutant strains, followed by diploid sporulation, tetrad analysis, and selection of the mutant combinations.

Microarray analyses

RNA purification, microarray characteristics, and other experimental steps, as well as data analyses, have been described previously (Ferrezuelo *et al*., 2009).

Isolation of vacuolar fraction

Isolation of vacuoles was based on the method described by Li *et al*. (2001), with modifications. About 10^{10} cells from an exponentially growing culture were centrifuged, resuspended in 30 ml of 0.1 M Tris-H_2SO_4 buffer, pH 9.3, with 10 mM DTT, and incubated at 30°C for 30 min. After two washings with 20 mM potassium phosphate buffer, pH 7.4, with 1.2 M sorbitol, cells were resuspended in 4 ml of this buffer containing Zymolyase 20T (Seikagaku Corp., Tokyo, Japan; at 3 mg/g of cells). Spheroplast formation was followed microscopically, and, once formed, spheroplasts were recovered by low-speed centrifugation (1800 × *g*, 5 min) and resuspended in 3.5 ml of a solution of 15% Ficoll (Sigma, St. Louis, MO) in 10 mM 1,4-piperazinediethanesulfonic acid (PIPES)–KOH, pH 6.8, plus 0.2 M sorbitol. After addition of DEAE-dextran (50 μg/ml, final concentration), the spheroplast lysate was kept for 2 min at 0°C and then for 5 min at 30°C with mild shaking. Magnesium chloride was added at a final concentration of 1.5 mM; the lysate was transferred to a centrifuge tube and then overlaid with 3 ml of the PIPES/sorbitol buffer with 8% Ficoll, 4 ml of buffer with 4% Ficoll, and 1 ml of buffer alone. Samples were centrifuged at 110,000 × g for 90 min with a Beckman SW55Ti rotor. Fractions of 0.4 ml were taken, an aliquot of each was separated for acetone precipitation of proteins, followed by Western analysis of compartment reporters (CPY for vacuole, porin for mitochondria, and hexokinase 1 for cytosol), and the remainder of each fraction was kept for phosphate determination. Vacuolar fraction was collected at the 0/4% Ficoll interphase.

Determination of intracellular ion levels

Cytosolic Ca^{2+} concentration was determined using the pentapotassium salt of indo-1 as described in Halachmi and Eilam (1989), after determining the fluorescence ratio at 410/480 nm according to Grynkiewicz *et al*. (1985). In this method, indo-1 (Sigma) is loaded in the cytosolic compartment by incubating the yeast cells at an acidic pH. To determine intracellular total Ca^{2+} levels (including membranous vesicles stores), cellular membranes were permeabilized with DEAE-dextran (2 mg/ml) as described in Halachmi and Eliam (1989).

Free Ca^{2+} levels at the ER lumen were determined using a specifically ER targeted version of aequorin, as described by Strayle *et al*. (1999). The protocol reported in the original work was essentially used, except that light emission was measured in a liquid suspension of cells and colenterazine n (Anaspec, Fremont, CA) was used as prosthetic group. Light recording was done before and after refilling with 1 mM $CaCl_2$. Subsequent cell lyses with 0.1% digitonin plus addition of 10 mM $CaCl_2$ allowed confirmation that previous measurements had been done in nonlimiting conditions for aequorin (Strayle *et al*., 1999).

Orthophosphate was measured by molybdate reactivity (Reddi *et al*., 2009). For determination of total intracellular phosphate, samples were treated with 1 N sulfuric acid for 10 min at 100°C before analysis. Polyphosphate levels were calculated as the difference between total P_i and orthophosphate levels.

Northern blot analyses

RNA isolation and electrophoresis, probe labeling with digoxigenin, hybridization, and signal detection were done as described previously (Bellí *et al*., 1998a). Gene probes were generated by PCR from genomic DNA, using oligonucleotides designed to amplify internal open reading frame sequences. *SNR19* mRNA was used as loading control. Signals were quantified using the ChemiDoc Imaging System (Bio-Rad, Hercules, CA) software. Background values were determined for a region lacking visible signal of the same size as the measured band and adjacent to it, and such background was subtracted for the respective band signal value.

Pulse-chase labeling and immunoprecipitation of CPY

Samples (~6×10^8 cells) from cultures in SC medium were resuspended in 10 ml of the same medium lacking methionine and cysteine and incubated for 30 min at the appropriate temperature before adding 500 µCi of a [^{35}S]methionine/[^{35}S]cysteine cocktail (Perkin Elmer, Waltham, MA). After a 5- or 6-min pulse, cold methionine and cysteine were added at 2 mM final concentration each. At successive 7-min intervals, samples of 1.5 ml were taken, and 20 mM (final concentration) sodium azide was added. Cells were pelleted, resuspended in 100 µl of lysis buffer (50 mM Tris-HCl, pH 7.5, 1 mM EDTA, 1% SDS, 6 M urea, and 1× protease inhibitor complete [Roche, Basel, Switzerland]) and lysed with glass beads by shaking and treatment at 100°C. The supernatant was carefully taken, and IP buffer (50 mM Tris-HCl, pH 7.5, 1 mM EDTA, 150 mM NaCl, 0.5% Tween-20, and 1× protease inhibitor complete) was added to a 1-ml final volume. The suspension was mixed with 50 µl of sheep anti-mouse immunoglobulin Dynabeads (Invitrogen, Carlsbad, CA) coupled to 3 µγ of mouse monoclonal anti-CPY antibodies (Molecular Probes, Carlsbad, CA). After mixing for 2 h at 4°C, the supernatant was eliminated and the beads were washed three times with 350 µl of IP buffer and then eluted with 20 µl of 1× Laemmli buffer, boiled, and separated by SDS–PAGE. Gels were autoradiographed, and x-ray film signals were quantified with ImageJ software (National Institutes of Health, Bethesda, MD).

Measurement of ER redox state

Real-time ER redox measurements were done as described in Merksamer *et al*. (2008) in cultures of transformants with plasmid pPM28, which expresses a redox-sensitive ero-GFP form.

Western blot analyses

Western blot analyses were done as described in Bellí *et al*. (1998b). The following primary antibodies were used: mouse monoclonal anti-CPY (1:500), rabbit polyclonal anti-Hxk1 (1:5000; USBiological, Salem, MA), or mouse monoclonal anti-porin (1:1000; Molecular Probes).

Determination of β-galactosidase activity

Enzyme activity (Miller units) was determined in permeabilized cells as described in Ausubel *et al*. (1987).

Statistical analyses

The Mann–Whitney *U* test was used, using the software JMP 10. Unless otherwise indicated, values in the mutant strains were compared with those of wild-type cells. *,**,***$p < 0.05$, 0.01, 0.001, respectively.

ACKNOWLEDGMENTS

J.P. is the recipient of a predoctoral grant from the University of Lleida. This work was supported by Grants BFU2010-17656 (Ministerio de Economía y Competitividad, Spain) and 2009/SGR/196 (Generalitat de Catalunya). We acknowledge the help of Francisco Ferrezuelo in the transcriptome analyses, the gift of biological material by Hans Rudolph (University of Stuttgart, Stuttgart, Germany), and the technical help of Sílvia Porras and Meritxell Martin.

REFERENCES

Antebi A, Fink GR (1992). The yeast Ca2+-ATPase homologue, *PMR1*, is required for normal Golgi function and localizes in a novel Golgi-like distribution. Mol Biol Cell 3, 633–654.

Ariño J, Ramos J, Sychrová H (2010). Alkali metal cation transport and homoestasis in yeasts. Microbiol Mol Biol Rev 74, 95–120.

Ausubel FM, Brent R, Kingston RE, Moore DD, Seidman JG, Smith JA, Struhl K (eds.) (1987). Current Protocols in Molecular Biology, New York: Wiley Interscience.

Beeler T, Gable K, Zhao C, Dunn T (1994). A novel protein, CSG2p, is required for Ca^{2+} regulation in *Saccharomyces cerevisiae*. J Biol Chem 269, 7279–7284.

Bellí G, Garí E, Aldea M, Herrero E (1998a). Functional analysis of yeast essential genes using a promoter-substitution cassette and the tetracycline-regulatable dual expression system. Yeast 14, 1127–1138.

Bellí G, Garí E, Piedrafita L, Aldea M, Herrero E (1998b). An activator/repressor dual system allows tight tetracycline-regulated gene expression in budding yeast. Nucleic Acids Res 26, 942–947.

Berndt C, Lillig CH, Holmgren A (2008). Thioredoxins and glutaredoxins as facilitators of protein folding. Biochim Biophys Acta 1783, 641–650.

Bonilla M, Cunningham KW (2003). MAP kinase stimulation of Ca^{2+} signaling is required for survival of endoplasmic reticulum stress in yeast. Mol Biol Cell 14, 4296–4305.

Bonilla M, Nastase KK, Cunningham KW (2002). Essential role of calcineurin in response to endoplasmic reticulum stress. EMBO J 21, 2342–2353.

Chakravarthi S, Jessop CE, Bulleid NJ (2006). The role of glutathione in disulphide bond formation and endoplasmic-reticulum-generated oxidative stress. EMBO Rep 7, 271–275.

Clapham DE (2007). Calcium signaling. Cell 131, 1047–1058.

Cohen Y, Megyeri M, Chen OC, Condomitti G, Riezman I, Loizides-Mangold U, Abdul-Sada A, Rimon N, Riezman H, Platt FM, *et al*. (2013). The yeast P5 type ATPase, Spf1, regulates manganese transport into the endoplasmic reticulum. PLoS One 8, e85519.

Cronin SR, Rao R, Hampton RY (2002). Cod1p/Spf1p is a P-type ATPase involved in ER function and Ca^{2+} homeostasis. J Cell Biol 157, 1017–1028.

Cunningham KW (2011). Acidic calcium stores of *Saccharomyces cerevisiae*. Cell Calcium 50, 128–139.

Cunningham KW, Fink GR (1996). Calcineurin inhibits VCX1-dependent H^+/Ca^{2+} exchange and induces Ca^{2+} ATPases in *Saccharomyces cerevisiae*. Mol Cell Biol 16, 2226–2237.

Cuozzo JW, Kaiser CA (1999). Competition between glutathione and protein thiols for disulphide-bond formation. Nat Cell Biol 1, 130–135.

Cyert MS (2003). Calcineurin signaling in *Saccharomyces cerevisiae*: how yeast go crazy in response to stress. Biochem Biophys Res Commun 311, 1143–1150.

Cyert MS, Philpott CC (2013). Regulation of cation balance in *Saccharomyces cerevisiae*. Genetics 193, 677–713.

Demaegd D, Foulquier F, Colinet AS, Gremillon L, Legrand D, Mariot P, Peiter E, Van Schaftinger E, Matthijs G, Morsomme P (2013). Newly characterized Golgi-localized family of proteins is involved in calcium and pH homeostasis in yeast and human cells. Proc Natl Acad Sci USA 110, 6859–6864.

Deponte M (2013). Glutathione catalysis and the reaction mechanisms of glutathione-dependent enzymes. Biochim Biophys Acta 1830, 3217–3266.

Dunn T, Gable K, Beeler T (1994). Regulation of cellular Ca^{2+} by yeast vacuoles. J Biol Chem 269, 7273–7278.

Durr G, Strayle J, Plemper R, Elbs S, Klee SK, Catty P, Wolf DH, Rudolf HK (1998). The medial-Golgi ion pump Pmr1 supplies the yeast secretory pathway with Ca^{2+} and Mn^{2+} required for glycosylation, sorting, and endoplasmic reticulum-associated protein degradation. Mol Biol Cell 9, 1149–1162.

Eide DJ, Clark S, Nair TM, Gehl M, Gribskov M, Guerinot ML, Harper JF (2005). Characterization of the yeast ionome: a genome-wide analysis of nutrient mineral and trace element homeostasis in *Saccharomyces cerevisiae*. Genome Biol 6, R77.

Ferrezuelo F, Aldea M, Futcher B (2009). Bck2 is a phase-independent activator of cell cycle-regulated genes in yeast. Cell Cycle 8, 239–252.

Frand AR, Kaiser CA (1998). The *ERO1* gene of yeast is required for oxidation of protein dithiols in the endoplasmic reticulum. Mol Cell 1, 161–170.

Gallogly MM, Mieyal JJ (2007). Mechanisms of reversible protein glutathionylation in redox signaling and oxidative stress. Curr Opin Pharmacol 7, 381–391.

Gietz RD, Sugino A (1988). New yeast-*Escherichia coli* shuttle vectors constructed with *in vitro* mutagenized yeast genes lacking six-base pair restriction sites. Gene 74, 3065–3073.

Goldstein AL, McCusker JH (1999). Three new dominant drug resistance cassettes for gene disruption in *Saccharomyces cerevisiae*. Yeast 15, 1541–1553.

Grynkiewicz G, Poenie M, Tsien RY (1985). A new generation of Ca^{2+} indicators with greatly improved fluorescence properties. J Biol Chem 260, 3440–3450.

Halachmi D, Eilam Y (1989). Cytosolic and vacuolar Ca^{2+} concentrations in yeast cells measured with the Ca^{2+}-sensitive fluorescence dye indo-1. FEBS Lett 256, 55–61.

Halachmi D, Eilam Y (1996). Elevated cytosolic free Ca^{2+} concentrations and massive Ca^{2+} accumulation within vacuoles, in yeast mutant lacking *PMR1*, a homolog of Ca^{2+}-ATPase. FEBS Lett 392, 194–200.

Herrero E, Bellí G, Casas C (2010). Structural and functional diversity of glutaredoxins in yeast. Curr Protein Pept Sci 11, 659–668.

Izquierdo A, Casas C, Mühlenhoff U, Lillig CH, Herrero E (2008). *Saccharomyces cerevisiae* Grx6 and Grx7 are monothiol glutaredoxins associated with the early secretory pathway. Eukaryot Cell 7, 1415–1426.

Kim S, Sideris DP, Sevier CS, Kaiser CA (2012). Balanced Ero1 activation and inactivation establishes ER redox homeostasis. J Cell Biol 196, 713–725.

Li X, Qian J, Wang C, Zheng K, Ye L, Fu Y, Han N, Bian H, Pan J, Wang J, Zhu M (2011). Regulating cytoplasmic calcium homeostasis can reduce aluminium toxicity in yeast. PLoS One 6, e21148.

Li Y, Camacho P (2004). Ca^{2+}-dependent redox modulation of SERCA 2b by ERp57. J Cell Biol 164, 35–46.

Li L, Chen OS, Ward DM, Kaplan J (2001). CCC1 is a transporter that mediates vacuolar iron storage in yeast. J Biol Chem 276, 29515–29519.

Lillig CH, Berndt C, Holmgren A (2008). Glutaredoxin systems. Biochim Biophys Acta 1780, 1304–1317.

Locke EG, Bonilla M, Liang L, Takita Y, Cunningham KW (2000). A homolog of voltage-gated Ca^{2+} channels stimulated by depletion of secretory Ca^{2+} in yeast. Mol Cell Biol 20, 6686–6694.

Martin DC, Kim H, Mackin NA, Maldonado-Báez L, Evangelista CC Jr, Beaudry VG, Dudgeon DD, Naiman DQ, Erdman SE, Cunningham KW (2011). New regulators of a high affinity Ca^{2+} influx system revealed through a genome-wide screen in yeast. J Biol Chem 286, 10744–10754.

Merksamer PI, Trusina A, Papa FR (2008). Real-time redox measurements during endoplasmic reticulum stress reveal interlinked protein folding functions. Cell 135, 933–947.

Mesecke N, Mittler S, Ecker E, Herrmann JM, Deponte M (2008a). Two novel monothiol glutaredoxins from *Saccharomyces cerevisiae* provide further insight into iron-sulfur cluster binding, oligomerization, and enzymatic activity of glutaredoxins. Biochemistry 47, 1452–1463.

Mesecke N, Spang A, Deponte M, Herrmann JM (2008b). A novel group of glutaredoxins in the *cis*-Golgi critical for oxidative stress resistance. Mol Biol Cell 19, 2673–2680.

Mouillon JM, Persson BL (2006). New aspects on phosphate sensing and signalling in *Saccharomyces cerevisiae*. FEMS Yeast Res 6, 171–176.

Oka OB, Bulleid NJ (2013). Forming disulfides in the endoplasmic reticulum. Biochim Biophys Acta 1833, 2425–2429.

Persson BL, Lagerstedt JO, Pratt JR, Pattison-Granberg J, Lundh K, Shokrollahzadeh S, Lundh F (2003). Regulation of phosphate acquisition in *Saccharomyces cerevisiae*. Curr Genet 72, 323–334.

Pollard MG, Travers KJ, Weissman JS (1998). Ero1p: a novel ubiquitous protein with an essential role in oxidative protein folding in the endoplasmic reticulum. Mol Cell 1, 171–182.

Raturi A, Ortiz-Sandoval C, Simmen T (2014). Redox dependence of endoplasmic reticulum (ER) Ca^{2+} signaling. Histol Histopathol 29, 543–552.

Reddi AR, Jensen LT, Naranuntarat A, Rosenfeld L, Leung E, Shah R, Culotta VC (2009). The overlapping roles of manganese and Cu/Zn SOD in oxidative stress protection. Free Radic Biol Med 46, 154–162.

Ruiz A, Serrano R, Ariño J (2008). Direct regulation of genes involved in glucose utilization by the calcium/calcineurin pathway. J Biol Chem 283, 13923–13933.

Sevier CS, Kaiser CA (2008). Ero1 and redox homeostasis in the endoplasmic reticulum. Biochim Biophys Acta 1793, 549–556.

Sherman F (2002). Getting started with yeast. Methods Enzymol 350, 3–41.

Stathopoulos AM, Cyert MS (1997). Calcineurin acts through the *CRZ1/TCN1*-encoded transcription factor to regulate gene expression in yeast. Genes Dev 11, 3432–3444.

Strayle J, Pozzan T, Rudolph HK (1999). Steady-state free Ca^{2+} in the yeast endoplasmic reticulum reaches only 10 mM and is mainly controlled by the secretory pathway pump Pmr1. EMBO J 18, 4733–4743.

Tanida I, Takita Y, Hasegawa A, Ohya Y, Anraku Y (1996). Yeast Cls2p/Csg2p localized on the endoplasmic reticulum membrane regulates a non-exchangeable intracellular Ca^{2+} pool cooperatively with calcineurin. FEBS Lett 379, 38–42.

Thewes S (2014). Calcineurin-Crz1 signaling in lower eukaryotes. Eukaryot Cell 13, 694–705.

Travers KJ, Patil CK, Wodicka L, Lockhart DJ, Weissman JS, Walter P (2000). Functional and genomic analyses reveal an essential coordination between the unfolded protein response and ER-associated degradation. Cell 101, 249–258.

Turano C, Gaucci E, Grillo C, Chichiarelli S (2011). ERp57/GRP58: a protein with multiple functions. Cell Mol Biol Lett 16, 539–563.

Vashist S, Frank CG, Jakob CA, Ng DTW (2002). Two distinctly localized P-type ATPases collaborate to maintain organelle homeostasis required for glycoprotein processing and quality control. Mol Biol Cell 13, 3955–3966.

Wach A, Brachat A, Pöhlmann R, Philippsen P (1994). New heterologous modules for classical or PCR-based gene disruptions in *Saccharomyces cerevisiae*. Yeast 13, 1793–1808.

Walter P, Ron D (2011). The unfolded protein response: from stress pathway to homeostatic regulation. Science 334, 1081–1086.

Weiner MP, Costa GL (1995). Rapid PCR site-directed mutagenesis. In: PCR Primer: a Laboratory Manual, ed. CW Dieffenbach and GS Dveksler, Cold Spring Harbor, NY: Cold Spring Harbor Laboratory Press, 613–621.

Yoshimoto H, Saltsman K, Gasch AP, Li HX, Ogawa N, Botstein D, Brown PO, Cyert MS (2002). Genome-wide analysis of gene expression regulated by the calcineurin/Crz1p signaling pathway in *Saccharomyces cerevisiae*. J Biol Chem 277, 31079–31088.

Yoshimura H, Tada T, Iida H (2004). Subcellular localization and oligomeric structure of the yeast putative stretch-activated Ca^{2+} channel component Mid1. Exp Cell Res 293, 185–195.

Zhao C, Beeler T, Dunn T (1994). Suppressors of the Ca^{2+}-sensitive yeast mutant (csg2) identify genes involved in sphingolipid biosynthesis. J Biol Chem 269, 21480–21488.

Zima AV, Blatter LA (2006). Redox regulation of cardiac calcium channels and transporters. Cardiovasc Res 71, 310–321.